Egypt. J. Chem. **Vol. 67,** No. 6 pp. 353 - 361 (2024)

Egyptian Journal of Chemistry

http://ejchem.journals.ekb.eg/

Mixed pd(II) complexes based on Cefadroxil drug: synthesis, characterization and biomedical applications

Lamis O. Abo baker[1], Abeer T. AbdEl-karim[2], Ahmed A. El-Sherif*[2], Walaa H. Mahmoud[2]

1 Basic Science Department, Modern Academy for Engineering and Technology, Egypt

2Department of Chemistry, Faculty of Science, Cairo University, Egypt

Abstract

Cefadroxil (Cef) plays a crucial role as a pharmaceutical agent in treating various ailments. Its widespread application in diverse pharmaceutical formulations has prompted the development of innovative Pd (II) coordination ternary metal complexes. These complexes are synthesized by employing Cefadroxil as the promising ligand, complemented by aromatic amines and bipyridine to form mixed ligands chelating compounds.

The stereochemical characteristics of these novel ternary metal complexes have been thoroughly investigated through a comprehensive analytical approach. This analysis encompasses elemental analysis, infrared spectroscopy (FT-IR), proton nuclear magnetic resonance (1H NMR) spectroscopy, determination of melting points, conductivity measurements, mass spectrometry, and thermal analysis techniques such as thermogravimetry (TG) and differential thermogravimetry (DTG). Through these methods, a detailed understanding of the structural attributes of the complexes has been attained, contributing to the advancement of knowledge in this field.

Moreover, the complexes were evaluated for their antimicrobial efficacy against various microorganisms, encompassing Gram-positive bacteria such as *Staphylococcus aureus* and *Streptococcus mutans*, Gram-negative bacteria including *Escherichia coli*, *Klebsiella pneumoniae*, and *Pseudomonas aeruginosa*, as well as fungi like *Candida albicans*, *Aspergillus Niger*, and *Aspergillus Ochraceous*. The assessment included a comparison with established benchmarks in the field, namely Ampicillin and Gentamicin for antibacterial activity, and Nystatin for antifungal activity. Furthermore, the paper delves into the anticancer attributes of the ligands and their respective metal complexes through viability assays targeting human cancer cells (MCF-7 cells). Notably, the Pd (II) ternary complexes exhibited significant potential as anti-Alzheimer's agents. The synthesized palladium complexes, displaying a pronounced selectivity for acetylcholinesterase (AChE), merit further exploration as promising candidates for addressing early-stage Alzheimer's disease symptoms..

Keywords:

Cefadroxil drug, Aromatic amines, Antimicrobial activity, anticancer activity, anti-alzahimar drugs, Complexes.

1. Introduction

Cefadroxil, the para hydroxyl derivative of cefalexin, exhibits antibacterial activity comparable to cefalexin and cefradine against various clinically isolated bacteria. Similar to cephalosporins, certain antibiotics, including cefadroxil, can form chelates with metal ions through electron donor groups or atoms. This interaction may lead to reduced intestinal absorption of these antibiotics due to the formation of chelate.

Cefadroxil demonstrates limited solubility in water but is soluble in alcohol and ether.[1] The efficacy of its antibacterial activity relies on the presence of the ß-lactam functionality, which can undergo hydrolysis under aqueous conditions. [2-3]

Considering these characteristics, the synthesis of ternary complexes involving cefadroxil could provide valuable insights into its potential applications .[4,5] The assessment of the antimicrobial attributes of these complexes aims to validate their potential as efficacious therapeutic agents. The inclusion of amino acids from biological systems in palladium complexes is being investigated with the intention of minimizing adverse effects or augmenting the intracellular concentration of these complexes.[6,7] This strategic approach is anticipated to enhance the antitumor properties of the complexes [8]. By forming chelates, the lipophilicity of the drug is augmented, leading to an increase in drug efficacy. This enhancement is attributed to the improved permeability of the drug at the site of action.

Alzheimer's disease (AD) is the predominant cause of dementia in the elderly [9]. The primary approach to its treatment involves the use of cholinesterase inhibitors [2]. The pathogenesis of AD is linked to a decrease in acetylcholine, a crucial neurotransmitter for memory function [3]. Acetylcholinesterase (AChE) in the brain regulates acetylcholine activity by breaking it down into acetal. In AD, AChE activity tends to either remain stable or increase [7]. Although four cholinesterase inhibitors (tacrine, donepezil, rivastigmine, and galantamine) are approved by the US Food and Drug Administration, they are associated with undesirable side effects [10].

Metal ions play diverse roles in brain function, contributing to redox reactions, amyloid-β aggregation, and oxidative stress, which are central to AD pathogenesis [6]. Consequently, metal chelators are being explored as potential inhibitors of AChE and BuChE [4, 5]. In 1991,

*Corresponding author e-mail: aelsherif@sci.cu.edu.eg/ aelsherif72@yahoo.com

Receive Date: 14 November 2023, Revised Date: 03 December 2023; Accept Date: 15 December 2023

DOI: 10.21608/EJCHEM.2023.248787.8876

©2024 National Information and Documentation Center (NIDOC)

Mital et al. reported the synthesis of palladium (II) complexes incorporating 1,10-phenanthroline and amino acids. Their research indicated that [Pd(phen)(valine)]Cl_2.H_2O exhibited a lower IC50 value against sarcoma P388 lymphocytic leukemia cells compared to cisplatin [8]. More recently, we have presented our research on the synthesis, characterization, biological activities, and the anticancer and anti-Alzheimer's properties of specific ternary Pd (II) complexes.

Materials and methods

2. Experimental

2.1.1. Chemicals and reagents

We utilized chemicals of the highest analytical grade, ensuring optimal purity for all experiments. The substances employed included N-benzylethylenediamine ($C_9H_{14}N_2$), picolyl amine ($C_6H_8N_2$), Bipyridine ($C_{10}H_8N_2$) from Sigma-Aldrich, and cefadroxil ($C_{16}H_{19}N_3O_5S.2H_2O$). Key reagent K2PdCl4 was sourced from Merck. Organic solvent-based processes involved ethyl alcohol (99%) and dimethylformamide (DMF). Deionized water from glass equipment was consistently used in all preparations.

Our research involved the breast tumor cell line MCF7, acquired from the American Type Culture Collection, stored in liquid nitrogen (-180°C). Preservation, maintenance, and subculturing of these tumor cell lines occurred at the National Cancer Institute in Cairo, Egypt.

2.1.2. Solutions

To generate new stock solutions of mixed ligand complexes at a concentration of 1×10^{-3} M, we accurately measured and dissolved the chelates in an appropriate volume of DMF. Following this, we assessed the conductivities of these solution complexes. The metal salt solutions utilized in our experiments underwent standardization using established and recommended procedures [8, 11].

2.1.3. Instrumentation

We performed elemental analyses of carbon, hydrogen, and nitrogen utilizing a CHNS932 (LECO) Vario Elemental analyzer at Cairo University's Microanalytical Center in Egypt. Melting point measurements were conducted using a triforce XMTD-3000 apparatus. Fourier transform infrared (FT-IR) spectra were captured using a Perkin-Elmer 1650 spectrometer over the 4000–400 cm−1 range, employing KBr disks as the medium. 1H NMR spectra in dimethyl sulfoxide-d6 (DMSO-d6) solutions were recorded at room temperature with a 300-MHz Varian-Oxford Mercury spectrometer, utilizing tetramethylsilane as an internal standard. Molar conductivity assessments of solid complex solutions at a concentration of 10−3 M in ethanol were carried out using a Jenway 4010 conductivity meter. Mass spectra, obtained via the electron ionization technique at 70 eV, were recorded using an MS-5988 GS-MS Hewlett-Packard instrument, located at Cairo University's Microanalytical Center. Antimicrobial assays were performed at the same center.

Anticancer activity experiments were conducted at Cairo University's National Cancer Institute, specifically in the Department of Cancer Biology and the Department of Pharmacology. Optical density (OD) measurements for each well were determined spectrophotometrically at 564 nm using an enzyme-linked immunosorbent assay (ELISA) microplate reader (Meter Tech. R960, USA).

The assessment of anti-Alzheimer's activity, focusing on butyrylcholinesterase (BuChE) inhibition, was carried out at Al-Azhar University's Biotechnology Research Center.

1.1. procedure

1.1. Abstra

Synthesis of the metal complexes

To synthesize mixed ligand complexes of palladium with aromatic amines and bipyridine using a 1:1 metal-to-amine molar ratio, the following procedure was employed Initially,K_2PdCl_4 was dissolved in dist water under stiring and heating up to $50c^0$. Subsequently, the aromatic amine was slowly added drop by drop to the filtered solution at a 1:1 ratio. The resulting precipitates were filtered, and the obtained solids, varying in color from yellow to brown, were dried under vacuum conditions.

In the case of mixed ligand complexes involving Cefadroxil, the preparation proceeded as follows: A mixture of binary complexes (Pd:amine) (Pd: bipyridine) was dissolved (1 mmol in 10 ml of DMF) and heated with stirring. Cefadroxil solution (1 mmol in 15 ml of distilled water) was then promptly added, and the stirring process continued for 3 hours. This yielded ternary complexes with molar ratios of 1:1:1 for the metal, amine or bipyridine and Cefadroxil. The resulting dark brown complexes were filtered, washed with ethanol, and subsequently dried under vacuum conditions. The specific yields of each complex are provided in Table 1.

1.2. Antimicrobial activity

The in vitro assessment of the antibacterial and antifungal properties of Ampicillin, Gentamicin, and Nystatin was conducted using the disc diffusion technique. These compounds served as positive controls for Gram-positive bacteria, Gram-negative bacteria, and fungi, respectively [12, 13]. The bacterial strains employed included Gram-positive bacteria such as *Staphylococcus aureus* and *Streptococcus mutans*, Gram-negative bacteria including *Escherichia coli, Klebsiella pneumonia*, and *Pseudomonas aeruginosa*, as well as fungal strains like *Candida albicans*, *Aspergillus Niger*, and *Aspergillus Ochraceous*.

To prepare the stock solutions (1 mmol), the ligands and their complexes were dissolved in DMSO. For the antibacterial activity assessment, a nutrient agar medium was prepared, cooled to 47°C, and inoculated with microorganisms. Once solidified, 5-mm-diameter holes were created using a sterile cork borer. The investigated compounds, dissolved in DMSO at 1×10−3 M, were added to Petri dishes (only 0.1 m). Subsequently, the bacterial and fungal growth plates were incubated for 20 hours at 37°C. Inhibition zones were then measured in millimeters, using a sterile cork borer. The antimicrobial activity experiments were conducted in triplicate, and the average of the final readings was determined to assess the antimicrobial activity [14].

1.3. Antitumor activity

The assessment of potential cytotoxicity for the compounds was conducted following the methodology described by Skehan and Storeng [15]. Initially, a 96-multiwell plate was utilized, with 10,000 cells seeded per well and allowed to attach for 24 hours. Subsequently, various concentrations of the compounds (ranging from 0, 5, 12.5, 25, 50, to 100 µg/mL) were introduced to the cell monolayer, with triplicate wells established for each concentration. The cells were then subjected to a 48-hour incubation period at 37°C and 5% CO2.

After the incubation, the cells underwent fixation, washing, and staining with sulforhodamine B. Excess stain was eliminated using acetic acid, and the stain adhering to the cells was recovered with a Tris-EDTA buffer. The optical density (OD) of each well was measured at 564 nm using an ELISA microplate reader. Subsequently, the mean background absorbance was automatically subtracted, and the mean values for each drug concentration were computed.

To depict the survival curve of the breast tumor cell line for each compound, the relationship between the surviving fraction and the drug concentration was plotted. The cell survival percentage was determined using the formula:

Survival fraction =

(OD of treated cells) / (OD of control cells)] The IC50 values, indicative of the concentrations required to achieve 50% inhibition of cell growth, were determined through this analysis. The experiment was repeated three times to ensure the consistency and reliability of the results.

G. Butyrylcholinesterase Activity Assay and Inhibition Studies (Anti-Alzhaimar activity).

The investigation focused on the hydrolysis of butyrylthiocholine iodide (BTC) by butyrylcholinesterase (BChE) within a MOPS buffer (50 mM, pH 8) at 25°C, employing spectrophotometry. The assessment, based on the Ellman method [15], involved the addition of 5, 5'-dithiobis-2-nitrobenzoic acid (DTNB) at a concentration of 0.125 mM. BChE (0.2 U/mL) initiation triggered the reactions, and the continuous monitoring of absorbance increase at 405 nm occurred using a Biosystem-310 spectrophotometer.

Enzyme activity determination involved analyzing the linear segments of the progress curves during the initial 60-second period. An extinction coefficient of 14.2 mM−1/cm−1 was applied.

For the exploration of BChE inhibition, varying concentrations of 1, 9-dimethyl-methylene blue (DMMB) were introduced into the reaction mixture (final volume 1.2 mL) [16]. It is noteworthy that the presence of methanol (≤1.25% (v/v)) in the reaction mixture did not influence enzyme activity.

Results and Discussion

Elemental analyses and molar conductivity measurements.

The ternary complexes of cefadroxil exhibit stability in atmospheric conditions. They demonstrate practical solubility in polar organic solvents such as ethanol (EtOH), methanol (MeOH), dimethylformamide (DMF), and dimethyl sulfoxide (DMSO), while being insoluble in water. The stoichiometry and composition of the cefadroxil(L) ligand and its metal complexes were confirmed through elemental analysis, wherein the metal/ligands ratio was determined to be 1:1:1 in the complexes. This ratio was established by estimating the metal contents, as well as carbon, hydrogen, nitrogen, and chlorine contents, as presented in Table 1.

The elemental analyses of both the ligand and its complexes are in good accordance with the proposed structures.

Molar conductivity values (Λm) of the mixed ligand complexes in DMF (10−3 M) at 25 ± 2°C were observed to be 78, 83, and 86 Ω^{-1} mol^{-1} cm^{2} for complexes 1, 2, and 3, respectively. These values suggest the electrolytic nature of the complexes, indicating the presence of anions in the outer coordination sphere. A summary of the results is provided in Table 1.

IR spectra

In order to clarify the mode of bonding and the metal complexes, the IR spectra of the free ligand and metal chelates were studied (Table 2 and Fig.1) and assigned on the basis of the careful comparison of their spectra with that of the free ligand (cefadroxil)

The free cefdroxil drug spectrum reveals distinctive bands, including a prominent peak at approximately 3219 cm−1, corresponding to the stretching vibration (ν(NH)) of NH groups. Notably, strong absorption bands at 1757 and 1686 cm−1 are assigned to the carbonyl of lactam (C=O) and the (C=O) amide stretching vibrations, respectively. Additional bands at 1563 cm−1 and 1399 cm−1 are associated with the asymmetrical and symmetrical stretching vibrations of COO^{-} carboxylate groups. The intense absorption band at 1267 cm−1 is attributed to the stretching vibration of tertiary N.

Upon the formation of ternary complexes, the sym(COO^{-}) band shifts to higher frequencies (approximately 47–64 cm−1), suggesting the involvement of the carboxylic group in metal ion coordination. Moreover, the carboxylate asymmetrical stretching band at 1563 cm–1 shifts to higher frequencies (about 14–44 cm−1), possibly indicating bond stabilization. Conversely, the band at 1267 cm−1 corresponding to ternary-N experiences a lower frequency shift (approximately 112–99 cm−1) compared to the ligand, hinting at a shift in electron density from the donor nitrogen (-N).[18]

Confirmation of metal-ligand bonding is evident in the spectra of the ternary complexes, as indicated by bands at 455–472 cm−1 (M–N) and 534–568 cm−1 (M–O), confirming the bonding of nitrogen and oxygen atoms from ligand groups to the metal cation. The solid complexes' IR spectra exhibit a broad band at 3424–3420 cm−1, attributed to the stretching vibration (ν(OH)) of hydroxyl groups. [17].

Mass spectra.

The mass spectra of the ternary complexeswere evaluated at 70 eV in electron ionization mode.

(1) The mass spectrum of the ternary complex involving cefadroxil(N-benzylethylenediamine)Pd chloride$2H_2O$ revealed three significant fragments. The initial peak at m/z 691.2 (attributed to the ternary complex with a calculated mass of 691 g/mol), the second peak at m/z 364 (M+1) indicating the presence of the second ligand cephardine (calculated

mass 363 g/mol), and the third peak at m/z 151.2 (M+1) indicating the presence of the first ligand (N-benzylethylenediamine) (calculated mass 150 g/mol). These findings align with the proposed molecular weight of the newly synthesized (1:1:1) metal:ligand 1:ligand 2 stoichiometric ratio. [19]

(2) The mass spectrum of the ternary complex involving cefadroxil(picolyl amine)Pd chloride$2H_2O$ exhibited three key fragments. The initial peak at m/z 650 (M+2) (calculated mass 648 g/mol), the second peak at m/z 363 indicating the presence of the second ligand cephardine (calculated mass 363 g/mol), and the third peak at m/z 108 indicating the presence of the first ligand e(picolyl amine) (calculated mass 108 g/mol). These observations support the proposed molecular weight and stoichiometric ratio of (1:1:1) for the newly synthesized complex.

Table. 1. show the physical and analytical data of the palladim Ternary Complexes

Compound	Color Yield (%)	M.p. (°C)	Found (Calcd)					A_m (Ω^{-1} mol^{-1} cm^2)
			C (%)	H (%)	N (%)	S (%)	M (%)	
[Pd(N ben)cef]Cl.2H$_2$O	Brown (87)	210	43.12 (43.41)	4.78 (4.92)	10.01 (10.13)	4.61 (4.63)	15.03 (15.40)	78
[Pd(pic)cef]Cl.2H$_2$O	Brown (88)	225	40.74 (40.36)	4.32 (4.10)	10.80 (10.27)	4.94 (4.78)	16.42 (16.23)	83
[Pd(Bipy)cef] Cl.2H$_2$O	Brown (78)	215	44.78 (44.37)	4.16 (4.03)	10.04 (9.89)	4.59 (4.32)	15.26 (15.03)	86

Table 2. IR spectral of the cefadroxil and palladim Ternary Complexes as follows

Compound	N N–H	υ(co) lactum	υ(co) amide	υ(coo) Asymmetric	υ(coo) symmetric	Tertiary N	υ(M-O)	υ(M-N)
Cefadroxil	**3219 sh**	**1757 m**	**1686 m**	**1563 sh**	**1399 sh**	**1267 m**	-	-
[Pd(N ben)cef]Cl.2H$_2$O	**3222 m**	1755 m	1680 m	1577 w	1446 m	1155 s	565 w	455 w
[Pd(pic)cef]Cl.2H$_2$O	3220 m	1755 m	1684 m	1604 s	1466 s	1168 s	568 w	461 w
[Pd(Bipy)cef] Cl.2H$_2$O	3218 m	1756 m	1685 m	1607 s	1463 s	1169 s	534 w	472 w

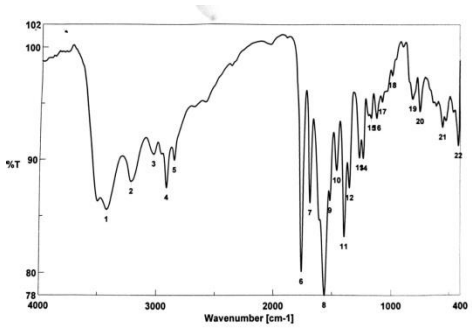

(1)

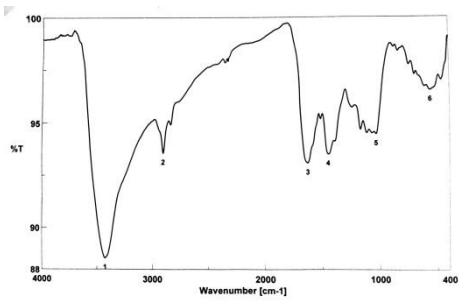

(2)

(3) [Pd(pic)cef]Cl.2H$_2$O,(4) Pd(Bipy)cef] Cl.2H$_2$O

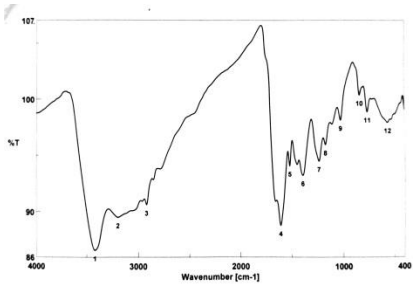

(3)

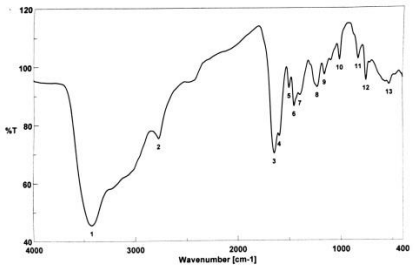

(4)

Figur 1. IR spectra of cefadroxil and its complexes ,(1) cefadroxil ,(2) [Pd(N ben)cef]Cl.2H$_2$O,

(3) The mass spectrum of the ternary complex involving cefadroxil(Bipyridine)Pd chloride $2H_2$**O** displayed three crucial fragments. The initial peak at m/z 698 (M+1) (calculated mass 697 g/mol), the second peak at m/z 363 indicating the presence of the second ligand cephardine (calculated mass 363 g/mol), and the third peak at m/z 156 indicating the presence of the first ligand (Bipyridine) (calculated mass 156 g/mol). These results are consistent with the proposed molecular weight and stoichiometric ratio of (1:1:1) for the newly synthesized complex.[20,21]

Thermal analyses.

The thermal characteristics of ternary complexes were assessed through thermogravimetric analysis within a temperature range of 10 ◦C to 800 ◦C under inert atmospheric conditions, employing a heating rate of 5 ◦C/min. The table provides information on temperature intervals and the corresponding proportion of mass reduction in the ternary complexes. The observed weight loss can be attributed to the removal of uncoordinated water chelates and coordinated molecules. The reliability of the results was confirmed by their consistency with the data obtained from the basic analysis.

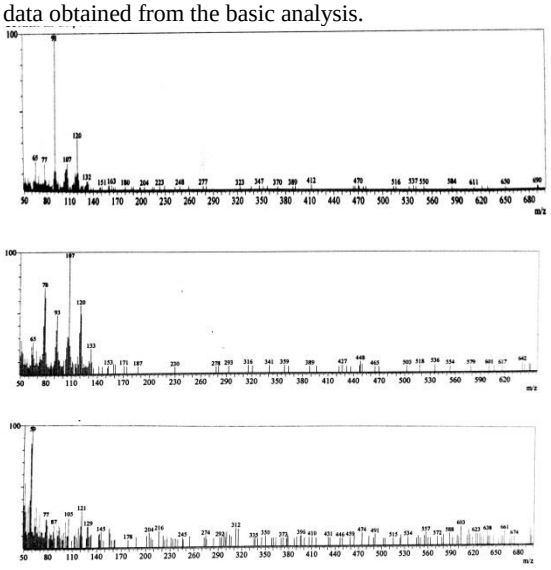

Figur 2.mass spectra of cefadroxil and its complexes
(a) [Pd(N ben)cef]Cl.2H_2O
(b) [Pd(pic)cef]Cl.2H_2O
(c) Pd(Bipy)cef] Cl.2H_2O

The findings align with the information derived from the fundamental analysis, indicating a correlation between the two sets of data. The ultimate mass loss is a consequence of the breakdown of residual carbon atoms and residual metal oxide. [17,18]

The TG thermal analysis of the ternary complex (1) with the general formula [PdL1L2]Cl·2H2O (where L1 = N-benzylethylenediamine, L2 = cefadroxil) revealed a two-step decomposition process, supported by corresponding data. The initial stage occurred in the temperature range of 42–125 °C, with a peak temperature at 83 °C. This stage was associated with the loss of two water molecules, resulting in a mass loss of 5.13% (calculated mass loss = 5.21%), indicating the removal of outer coordination water.

The subsequent decomposition stage took place in the temperature range of 350–670 °C, corresponding to the complete breakdown of a portion of the complex (C23H30ClN5O4S). This stage exhibited a mass loss of 73.34% (calculated mass loss = 73.44%), with the DTG curve showing peak temperatures at 405 and 538 °C. Finally, at 800 °C, the mass residue decomposition was attributed to the formation of PdO + 2C, resulting in a total weight loss of 78.47% (calculated 78.65%).

The thermal analysis of the ternary complex (2) with the general formula [Pd L1 L2]Cl·2H2O, where L1 is picolyl amine and L2 is cefadroxil, revealed four distinct weight loss events. In the initial stage, occurring between 25 and 101 °C with a peak temperature at 57 °C, two water molecules were lost, resulting in a mass loss of 5.13% (calculated mass loss = 5.60%). This phenomenon suggests the release of outer coordination water.

The second decomposition stage, observed in the temperature range of 101-344 °C, corresponds to the complete decomposition of a portion of the complex (HCl, CO2, C7H11N2OH), with a mass loss of 34.01% (calculated mass loss = 33.50%). The DTG curve indicated a maximum peak temperature at 245 °C.

Subsequently, the third and fourth decomposition stages, occurring in the temperature range of 345-596 °C, signify the complete decomposition of another part of the complex (C14H14N3SO2), resulting in a mass loss of 45.36% (calculated mass loss = 45.8 0%). The DTG curve displayed maximum peak temperatures at 246 and 371 °C.

Table.5. Thermoanalytical results (TG and DTG) of the palladim Ternary Complexes are as follows

Complex	TG-range (°C)	DTG max	n*	Mass loss Estim (calcd)% (Total mass Loss)	Assignment	Residues
[Pd(N ben)cef]Cl.2H_2O	**(42-125)** **(350-670)**	**83** **405,538**	**1** **2**	**5.13(5.21)** **73.34(73.44)** **78.47(78.65)**	**Loss of 2H2O** **LOSS OF $C_{23}H_{30}N_5O_4SCl$**	**PdO+2C**
[Pd(pic)cef]Cl.2H_2O	**(25-101)** **(101-344)** **(345-595)**	**57** **245** **370,410**	**1** **1** **2**	**5.31 (5.60)** **34.01(33.50)** **45.36(45.8)** **84.68(84.90))**	**Loss of $2H_2O$** **Loss of HCl,CO_2,$C_7H_{11}N_2OH$** **LOSS OF $C_{14}H_{14}N_3SO_2$**	**PdO**
[Pd(Bipy)cef] Cl.2H_2O	**27-97** **98-167** **167-287** **287-425** **425-620**	**62.7** **135** **264** **287** **452**	**1** **1** **1** **1** **1**	**5.23 (5.16)** **6.35 (6.33)** **20.98 (20.73)** **22.72 (22.38)** **25.95 (25.53)** **81.23(80.13)**	**Loss of $2H_2O$** **Loss of CO** **Loss of HCl, C_6H_6NO** **Loss of, $C_{10}H_8N_2$** **Loss of $C_9H_{10}N_2S$**	**PdO**

Finally, at a temperature of 800 °C, the decomposition of the remaining mass residue led to the formation of PdO, contributing to a total weight loss of 84.68% (calculated 84.90%).

In the thermal analysis of the ternary complex (3) with the general formula [PdL1L2]Cl·2H2O, where L1 is bipyridine and L2 is cefadroxil, five distinct weight loss events were observed. The initial stage occurred in the temperature range of 27-97°C, reaching a maximum temperature of 62.7°C. This stage was associated with the elimination of two water molecules, resulting in a mass loss of 5.23% (calculated mass loss = 5.16%), indicating the removal of outer coordination water.

The second decomposition stage, spanning temperatures from 98 to 167°C, corresponded to the complete decomposition of a portion of the complex (CO), with a mass loss of 6.35% (calculated mass loss = 6.33%). The DTG curve exhibited a peak temperature at 135°C.

The third decomposition stage, occurring in the temperature range of 167-287°C, was attributed to the complete decomposition of another part of the complex (HCl, C6H6NO) and resulted in a mass loss of 20.98% (calculated mass loss = 20.73%). The DTG curve exhibited a peak temperature at 264°C.

The fourth decomposition stage, ranging from 287 to 425°C, indicated the complete decomposition of a component (C10H8N2) with a mass loss of 22.72% (calculated mass loss = 22.38%). The DTG curve reached its maximum peak temperature at 287°C.

The fifth and final decomposition stage occurred between 425 and 620°C, corresponding to the complete decomposition of another part of the complex (C9H10N2S) with a mass loss of 25.95% (calculated mass loss = 25.53%). The DTG curve exhibited a maximum peak temperature at 452°C.

Finally, at a temperature of 800°C, the decomposition of the remaining mass residue was attributed to PdO, resulting in a total weight loss of 81.23% (calculated 80.13%).[22,23]

^{1}HNMR spectra.

The structural analysis of the Cefadroxil ligand (L) and its mixed palladium (II) complexes was carried out using NMR data, as summarized in Table 3. The 1H NMR spectra of Cefadroxil (L) and its palladium complexes were recorded in DMSO-d6 with tetramethylsilane (TMS) as the internal standard. Several key observations were made:

In the 1H NMR spectrum of the Cefadroxil ligand, a singular peak at 9.02 ppm corresponding to C-OH (s) was identified. To confirm that this peak corresponds to the acidic group COOH, D2O solvent was introduced, leading to the disappearance of this band. In the ternary complexes 1, 2, and 3, this peak vanished due to the ionization of COO-, providing evidence for the coordination of Cefadroxil to the binary complex through COO-, acting as a uninegative bidendate ligand. This suggests that Cefadroxil coordinates to the metal ions by deprotonation, consistent with conclusions drawn from IR spectral data [25].

Furthermore, the ligand exhibited multiple signals in the range of 7.19-6.71 ppm (m) corresponding to aromatic protons. Singlet peaks were observed at 8.74 ppm for CH-NH2 (s), 8.27 ppm for CH-NH-CH (s), 5.68 ppm for CH-CH-NH (d), 5.21 ppm for S-CH-CH-NH (d), 4.86 ppm for CH-METHINE (d), 3.50 ppm for CH2-CH (s), and 2.06 ppm for CH3 (s).

In the case of the ternary complexes, a slight downfield shift was noted in the signals, attributed to the coordination of Cefadroxil to Pd (II) complexes [24, 25].

Table 5. **^{1}HNMR of cefdroxil and metal complexes**

Compound	Chemical shift, (δ) ppm	Assignment
Cefadroxil	**9.02**	**(s, H ,COOH)**
	9.60	**(s, H ,OH)**
	8.74	**(s,2H , CH-NH2)**
	8.27	**(s,H ,CH-NH-CH)**
	7.19- 6.71	**(m,5H,CH benzen)**
	5.68	**(d,H ,CH-CH-NH)**
	5.21	**(d,H ,S-CH-CH-NH)**
	4.86	**(S, H, CH METHINE)**
	3.50	**(d,2H ,CH2-CH)**
	2.06	**(s,3H ,CH3)**
Pd(N ben)cef]Cl.2H_2O	**Disappear**	**(s, H ,COOH)**
	9.70	**(s, H ,OH)**
	8.11	**(s,2H , CH-NH2)**
	7.80	**(s,H ,CH-NH-CH)**
	7.55-6.76	**(m,5H,CH benzen)**
	5.40	**(d,H ,CH-CH-NH)**
	5.18	**(d,H ,S-CH-CH-NH)**
	4.63	**(S, H, CH METHINE)**
	3.48	**(d,2H ,CH2-CH)**
	1.89	**(s,3H ,CH3)**
[Pd(pic)cef]Cl.2H_2O	**Disappear**	**(s, H ,COOH)**
	9.60	**(s, H ,OH)**
	8.65	**(s,2H , CH-NH2)**
	8.16	**(s,H ,CH-NH-CH)**
	7.76-6.75	**(m,5H,CH benzen)**
	5.43	**(d,H ,CH-CH-NH)**
	5.16	**(d,H ,S-CH-CH-NH)**
	4.63	**(S, H, CH METHINE)**
	3.38	**(d,2H ,CH2-CH)**
	2.1	**(s,3H ,CH3)**
[Pd(Bipy)cef] Cl.2H_2O	**Disappear**	**(s, H ,COOH)**
	9.77	**s, H ,OH)**
	8.69	**(s,2H , CH-NH2)**
	8.24	**(s,H ,CH-NH-CH)**
	7.08-6.08	**(m,5H,CH benzen)**
	5.70	**(d,H ,CH-CH-NH)**
	5.12	**(d,H ,S-CH-CH-NH)**
	3.41	**(S, H, CH METHINE)**
	2.74	**(d,2H ,CH2-CH)**
	2.63	**(s,3H ,CH3)**

Antimicrobial activity.

The assessed Pd(II) complexes were subjected to screening to evaluate their antimicrobial efficacy against a spectrum of bacterial and fungal strains, encompassing Gram-positive bacteria such as *Staphylococcus aureus* and *Streptococcus mutans*, Gram-negative bacteria including *Escherichia coli*, *Klebsiella pneumoniae*, and *Pseudomonas aeruginosa*, as well as fungi like *Candida albicans*, *Aspergillus Niger*, and *Aspergillus Ochraceous*.The antibacterial and antifungal properties were assessed using the disc diffusion method depicted in Fig.(3), and a summary of the outcomes is presented in

Table (6).The results indicate noteworthy activity of the investigated complexes against both Gram-positive and Gram-negative bacterial strains [27, 28]. Specifically, the Pd(pic)cef metal complexes exhibited robust antibacterial

effects against *Escherichia coli* (26.3±0.6), *Klebsiella pneumonia* (23.6±0.6*), Pseudomonas aeruginosa* (23.6±0.6), and antifungal activity against *Candida albicans* (27.3±0.6), *Aspergillus Nigar* (25.6±0.6), *Aspergillus Ochraceous* (22.3±0.6), surpassing the parent ligand and other complexes. Notably, the synthesized Pd(pic)ceph chloride complex demonstrated significantly heightened Gram-positive bacteria activities (*Staphylococcus aureus*) at 32.3±0.6 and superior antifungal activity against *Candida albicans*, *Aspergillus Nigar*, and *Aspergillus Ochraceous* compared to the parent ligand and other complexes. These heightened antibacterial and antifungal activities of the synthesized metal ligand complexes are ascribed to the chelation theory [29].

Anticancer activity

The synthesized complexes were assessed for their potential anticancer properties through cytotoxicity testing against the human breast cancer cell line, MCF7. The MTT colorimetric assay was employed to evaluate their anticancer activity after a 24-hour incubation period, and the results are summarized in Table 7 The findings indicated significant anticancer effects on MCF7 cells, with the extent of cell viability reduction correlating with increasing complex concentrations. Importantly, the complexation of the ligand with metal ions was found to enhance the anticancer activity (references [30,31]

The data in table 7 show that the cefradoxil have lowest cytotoxicity against MCF7 cells IC50 value**95.6,but the the chelating** give highter activity than the cefadroxil. ,in order of Pd(Bipy) > Pd(pic) > Pd(N ben) >[Pd(Bipy)cef] Cl.2H2O > [Pd(pic)cef]Cl.2H2O> [Pd(N ben)cef]Cl.2H2O

Among the various complexes tested, Pd(Bipy) demonstrated the highest cytotoxicity against MCF7 cells. Notably, the IC50 value for Pd(Bipy) was remarkably low, at 27.2µg/ml, underscoring its potent anticancer activity.

Anti-alzahimar activity

Acetylcholinesterase inhibitors have been widely employed in the treatment of neurodegenerative diseases. In a recent study, palladium mixed complexes were synthesized and tested for their ability to inhibit AChE. The Pd (pic) ceph chloride complex exhibited the most potent inhibitory activity against AChE, with an IC50 value of 6.01 µM. Conversely, the Cefadroxil (Bipyridine) Pd chloride complex demonstrated the weakest inhibitory activity, with an IC50 value of 15.06 µM. The data presented in the study clearly highlight that the primary factor influencing enzyme inhibition is the nature of the R substituent of the amine, emphasizing its crucial role in determining inhibitory potency [31].

Table. 6. Biological activity of palladium binary and ternary complexes

Compound		Inhibition zone diameter (mm / mg sample)							
		Gram positive bacterial		Gram negative bacterial species			Fungi		
		Staphylococcus aureus ATCC:13565)	*Streptococcus mutans ATCC:25175)*	*E.coli (ATCC:10536*	*Klebsiella pneumonia (ATCC:10031*	*Pseudomonas aeruginosa ATCC:27853)*	*Candida albicans ATCC:10231)*	*Asperagillus Nigar (ATCC:16404)*	*Asperagillus Ochraceous (ATCC:22947)*
Cefadroxil		**27.3±*0.6***	**26.3±*0.6***	***17.3±0.5***	***20.3±0.5***	**NA**	**NA**	**NA**	**NA**
Pd(N ben) binary		**22.6±*0.6***	**23.3±*0.6***	**23.3±*0.6***	**22.0±*0.1***	**17.3±*0.5***	**NA**	**NA**	**NA**
[Pd(N ben)cef]Cl.2H$_2$O		**13.6 ±*0.5***	**8.3 ±*0.5***	**NA**	**NA**	**NA**	**9.3±0.5**	***NA***	**NA**
Pd(pic) binary		**26.3±*0.6***	**23.3±*0.6***	**26.3±*0.6***	**23.6±*0.6***	**23.6±*0.6***	***27.3±0.6***	***25.6±0.6***	**22.3±*0.6***
[Pd(pic)cef]Cl.2H$_2$O		**32.3±*0.6***	**12.3±*0.5***	**8.6±0.5**	**9.3±0.5**	**NA**	***23.3±0.6***	***24.0±1.0***	***24.6±0.6***
Pd(Bipy) binary		**22.3±*0.6***	**20.3±*0.6***	**21.6±*0.6***	**21.3±*0.6***	**18.3±*0.6***	***NA***	***NA***	**NA**
[Pd(Bipy)cef] Cl.2H$_2$O		**NA**	**NA**	**NA**	**NA**	**NA**	**NA**	**NA**	**NA**
Standard	***Ampicillin***	***22±0.1***	***30±0.5***	-----	------	------	---------	---------	---------
	Gentamicin	--------	----------	***27±0.5***	***25±0.5***	***28±0.3***	--------	--------	----------
	Nystatin	--------	----------	----	----------	---------	***21±0.5***	***19±0.5***	**20.3-±*0.5*-----**

TABLE .7 Anticancer activity of palladium binary and ternary complexes against breast cancer .

samples	Concentration (µg/mL)				
	Surviving fraction (%)				
	12.5	25	50	100	IC50
Cefadroxil	80	77	62.2	48.7	95.6
Pd(N ben)binary	81	63	41	35	40
[Pd(N ben)cef]Cl.2H$_2$O	90.9	76.8	54	46	73.6
Pd(pic) binary	76	55	38	21	32
[Pd(pic)cef]Cl.2H$_2$O	89.3	61	40	36	71.4
Pd(Bipy) binary	74	52	31	20	27.2
[Pd(Bipy)cef] Cl.2H$_2$O	77	66	58	40	71

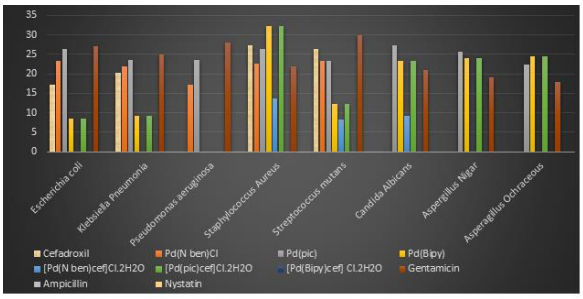

Figur 3. Biological activity of palladium binary and ternary complexes

References

1. 1.Synthesis, characterization and antimicrobial studies of schiff base transition metal complexes of Cr (II), Mn (II), Co (II), Ni (II), Zn (II) and Cd (II) derived from cefadroxil
2. Han, H. J., Lee, J. J., Park, S. A., Park, H. Y., Kim, J. E., Shim, Y. S., Shim, D.-S., Kim, E.-J., Yoon, S. J., & Choi, S. H. (2011). Efficacy and safety of switching from oral cholinesterase inhibitors to the rivastigmine transdermal patch in patients with probable Alzheimer's disease. *Journal of Clinical Neurology*, *7*(3), 137–142.
3. Adsersen, A., Kjølbye, A., Dall, O., & Jäger, A. K. (2007). Acetylcholinesterase and butyrylcholinesterase inhibitory compounds from Corydalis cava Schweigg. & Kort. *Journal of Ethnopharmacology*, *113*(1), 179–182.
4. J Bonda, D., Liu, G., Men, P., Perry, G., A Smith, M., & Zhu, X. (2012). Nanoparticle delivery of transition-metal chelators to the brain: oxidative stress will never see it coming! *CNS & Neurological Disorders-Drug Targets (Formerly Current Drug Targets-CNS & Neurological Disorders)*, *11*(1), 81–85.
5. Masoud, M. S., Ali, A. E., Ghareeb, D. A., & Nasr, N. M. (2013). Synthesis and characterization of cephradine metal complexes as Alzheimer disease therapeutic agent: an in vitro kinetic study on acetylcholinesterase and monoamine oxidase. *Chemical & Pharm. Res*, *5*(12), 1325–1334.
6. Budimir, A., Humbert, N., Elhabiri, M., Osinska, I., Biruš, M., & Albrecht-Gary, A.-M. (2011). Hydroxyquinoline based binders: Promising ligands for chelatotherapy?
7. Greig, N. H., Lahiri, D. K., & Sambamurti, K. (2002). Butyrylcholinesterase: an important new target in Alzheimer's disease therapy. International Psychogeriatrics, 14(S1), 77–91.
8. Vogel, A. I. (1962). A Text Book of Quantitative Inorganic Analysis Inlcuding Elementary Instrumental Analysis. English Language Book Society.
9. Small, G., & Bullock, R. (2011). Defining optimal treatment with cholinesterase inhibitors in Alzheimer's disease. *Alzheimer's & Dementia*, *7*(2), 177–184.
10. Mukherjee, P. K., Kumar, V., Mal, M., & Houghton, P. J. (2007). Acetylcholinesterase inhibitors from plants. *Phytomedicine*, *14*(4), 289–300.
11. Abdelkarim, A. T., Mahmoud, W. H., & El-Sherif, A. A. (2021). Potentiometric, thermodynamics and coordination properties for binary and mixed ligand complexes of copper (II) with cephradine antibiotic and some N-and O-bound amino acids (α-alanine and β-alanine). *Journal of Molecular Liquids*, *328*, 115334.
12. El-Said, A. I., Aly, A. A. M., El-Meligy, M. S., & Ibrahim, M. A. (2009). Mixed ligand zinc (II) and cadmium (II) complexes containing ceftriaxone or cephradine antibiotics and different donors. *Journal of the Argentine Chemical Society*, *97*(2), 149–165.
13. De, A., Ray, H. P., Jain, P., Kaur, H., & Singh, N. (2020). Synthesis, characterization, molecular docking and DNA cleavage study of transition metal complexes of o-vanillin and glycine derived Schiff base ligand. Journal of Molecular Structure, 1199, 126901.
14. Vural, H. (2022). A novel copper (II) complex containing pyrimidine-4-carboxylic acid: Synthesis, crystal structure, DFT studies, and molecular docking. *Journal of Molecular Structure*, *1265*, 133390.
15. Skehan, P., Storeng, R., Scudiero, D., Monks, A., McMahon, J., Vistica, D., Warren, J. T., Bokesch, H., Kenney, S., & Boyd, M. R. (1990). New colorimetric cytotoxicity assay for anticancer-drug screening. *JNCI: Journal of the National Cancer Institute*, *82*(13), 1107–1112.
16. Sezgin, Z., Biberoglu, K., Chupakhin, V., Makhaeva, G. F., & Tacal, O. (2013). Determination of binding points of methylene blue and cationic phenoxazine dyes on human butyrylcholinesterase. *Archives of Biochemistry and Biophysics*, *532*(1), 32–38.
17. Synthesis, characterization and electronic spectra of cefadroxil complexes of d-block elements M.A. Zayed∗, S.M. Abdallah Chemistry Department, Faculty of Science, Cairo University, Giza, A.R., Egypt Received 10 March 2003; accepted 25 November 2003Synthesis, characterization, molecular docking and DNA cleavage study of transition metal complexes of o-vanillin and glycine derived Schiff base ligand Anindita De* , Hari Prakash Ray, Preeti Jain, Harsimrut Kaur, Nikita Singh Department of Chemistry & Biochemistry, School of Basic Sciences and Research, Sharda University, Greater Noida, India
18. Tofiq, D. I., Hassan, H. Q., & Abdalkarim, K. A. (2021). Preparation of a novel Mixed-Ligand divalent metal complexes from solvent free Synthesized Schiff base derived from 2, 6-Diaminopyridine with cinnamaldehyde and 2, 2′-Bipyridine: Characterization and antibacterial activities. Arabian Journal of Chemistry, 14(12), 103429.
19. Aljahdali, M. S., & El-Sherif, A. A. (2020). Synthesis and biological evaluation of novel Zn (II) and Cd (II) Schiff base complexes as antimicrobial, antifungal, and antioxidant agents. *Bioinorganic Chemistry and Applications*, *2020*, 1–17.
20. I. Tofiq *, Hanar Q. Hassan, Karzan A. Abdalkarim (Shebl, 2017; Adly *et al*., 2019; Aljahdali and El-

Sherif, 2020).) Preparation of a novel Mixed-Ligand divalent metal complexes from solvent free Synthesized Schiff base derived from 2,6-Diaminopyridine with cinnamaldehyde and 2,20 - Bipyridine: Characterization and antibacterial activities Diary

21. El-Gammal, O. A., El-Bindary, A. A., Mohamed, F. S., Rezk, G. N., & El-Bindary, M. A. (2022). Synthesis, characterization, design, molecular docking, anti COVID-19 activity, DFT calculations of novel Schiff base with some transition metal complexes. *Journal of Molecular Liquids*, *346*, 117850.
22. Mir, M. A. (2022). Synthesis, Catalysis and Antimicrobial activity of 5d-metal chelate complex of Schiff base ligands. *Inorganic Chemistry Communications*, *142*, 109594.
23. Rajakkani, P., Alagarraj, A., & Thangavelu, S. A. G. (2021). Tetraaza macrocyclic Schiff base metal complexes bearing pendant groups: Synthesis, characterization and bioactivity studies. *Inorganic Chemistry Communications*, *134*, 108989.
24. Kargar, H., Torabi, V., Akbari, A., Behjatmanesh-Ardakani, R., Sahraei, A., & Tahir, M. N. (2020). Pd (II) and Ni (II) complexes containing an asymmetric Schiff base ligand: Synthesis, X-ray crystal structure, spectroscopic investigations and computational studies. *Journal of Molecular Structure*, *1205*, 127642.
25. El-Gammal, O. A., El-Bindary, A. A., Mohamed, F. S., Rezk, G. N., & El-Bindary, M. A. (2022). Synthesis, characterization, design, molecular docking, anti COVID-19 activity, DFT calculations of novel Schiff base with some transition metal complexes. *Journal of Molecular Liquids*, *346*, 117850
26. Emad S. Mousa, Walaa H. Mahmoud, Appl Organometal Chem. 33:e4844 (2019) 1-18.
27. De, A., Ray, H. P., Jain, P., Kaur, H., & Singh, N. (2020). Synthesis, characterization, molecular docking and DNA cleavage study of transition metal complexes of o-vanillin and glycine derived Schiff base ligand. Journal of Molecular Structure, 1199, 126901.
28. Sathyanarayana, D. N. (2001). Electronic absorption spectroscopy and related techniques. Universities Press.
29. Ghosh, A. K., Mitra, M., Fathima, A., Yadav, H., Choudhury, A. R., Nair, B. U., & Ghosh, R. (2016). Antibacterial and catecholase activities of Co (III) and Ni (II) Schiff base complexes. Polyhedron, 107, 1–8.
30. Grosdidier, A.; Zoete, V.; Michielin, O. SwissDock, a protein-small molecule docking web service based on EADock DSS. Nucleic Acids Res. 2011, 39, 270–277. [CrossRef] [PubMed]